El Niño: Catastrophe or Opportunity

LISA GODDARD AND MAXX DILLEY

International Research Institute for Climate Prediction, The Earth Institute of Columbia University, Palisades, New York

(Manuscript received 2 December 2003, in final form 3 June 2004)

ABSTRACT

El Niño–Southern Oscillation (ENSO) phenomenon, a periodic warming of sea surface temperatures in the eastern and central equatorial Pacific, generates a significant proportion of short-term climate variations globally, second only to the seasonal cycle. Global economic losses of tens of billions of dollars are attributed to extremes of ENSO (i.e., El Niño and La Niña), suggesting that these events disproportionately trigger socioeconomic disasters on the global scale. Since global El Niño/La Niña–associated climate impacts were first documented in the 1980s, the prevailing assumption has been that more severe and widespread climate anomalies, and, therefore, greater climate-related socioeconomic losses, should be expected during ENSO extremes. Contrary to expectations, climate anomalies associated with such losses are not greater overall during ENSO extremes than during neutral periods. However, during El Niño and La Niña events climate forecasts are shown to be more accurate. Stronger ENSO events lead to greater predictability of the climate and, potentially, the socioeconomic outcomes. Thus, the prudent use of climate forecasts could mitigate adverse impacts and lead instead to increased beneficial impacts, which could transform years of ENSO extremes into the least costly to life and property.

1. Introduction

The reported "cost" of El Niño events contributes greatly to misconceptions about the global climate effects and socioeconomic impacts of El Niño and La Niña. The estimated costs of the two largest El Niño events of the twentieth century were 8–18 billion U.S. dollars (USD) for the 1982/83 event (UCAR 1994; Sponberg 1999), and approximately 35–45 billion USD for the 1997/98 event (Sponberg 1999). But those figures neither refer to *increases* in economic losses, nor to losses from climate variability explicitly attributable to El Niño. Rather, they represent a gross estimate of all hydrometeorological impacts worldwide in those years. How these losses compare with those during ENSO-neutral periods has not been established. Furthermore, during El Niño events, El Niño is implicitly assumed be associated with all climate-related losses.

Natural disasters are loss events with socioeconomic as well as natural causes. Hazard events, including those related to climate, such as drought, floods, strong winds, and temperature extremes, constitute one group of causal factors. A second group of causal factors is the vulnerability characteristics of the exposed elements (i.e., people, infrastructure, and economic activities) that make them susceptible to damage from the occurrence of a specific type of hazard event. Impacts of climate anomalies are attenuated by the vulnerabilities of the exposed elements. Like climate, socioeconomic vulnerability varies over both space and time.

This study seeks to establish the degree to which ENSO events and disasters are related on two levels. The first level is to look for the signal of ENSO extremes in terms of disasters, because this often fuels the global anxiety surrounding ENSO events. In this line of inquiry, hazard exposure and vulnerability are confounding factors. Thus, the second level is to examine the effect of ENSO extremes on climate anomalies directly.

Using disaster data and climate data from both observations and predictions, three questions are considered: "To what extent do climate-related disasters increase during years of ENSO extremes?"; "Do climate anomalies become more severe or widespread during ENSO extremes?"; and "What is our ability to predict climate variations during ENSO extremes relative to other times?". This latter question addresses the potential to reduce negative climate-related impacts by reducing vulnerability to climatic hazards.

2. Data and methods

a. Disaster data

Currently, the only publicly available global disaster event database is the Emergency Disasters Data Base

Corresponding author address: Dr. Lisa Goddard, International Research Institute for Climate Prediction, The Earth Institute of Columbia University, 61 Route 9W, 228 Monell Bldg., Palisades, NY 10964-8000.
E-mail: goddard@iri.columbia.edu

(EM-DAT 2003), which is maintained by the Center for Research on the Epidemiology of Disasters in Brussels, Belgium. EM-DAT sources include United Nations (UN) agencies, nongovernmental organizations, insurance companies, research institutes, and press agencies. Criteria for inclusion in EM-DAT as a "reported disaster" includes exhibiting one or more of the following characteristics: 10 people killed, 100 people affected,[1] significant disaster (e.g., "second worst"), significant damage, and declaration of a state of emergency or/and appeal for international assistance. EM-DAT contains approximately 9000 natural disaster entries from 1900 to the present. Reporting is more consistent in recent decades, so that only approximately 7000 entries from 1975 onward are considered.

Given the availability of data in EM-DAT and the range of losses associated with climatic hazards, four variables are candidates to represent disasters in an analysis of El Niño/La Niña–related climate anomalies and disasters. These include disaster frequency, mortality, the number of affected people, and economic losses. Disaster frequency is based on a binary determination that a loss event occurred that exceeded EM-DAT's inclusion criteria. The other three variables—mortality, the number of affected people, and economic losses—require a more precise estimation of the magnitude of the losses.

Disaster frequency has several advantages, as well as one disadvantage, in the context of the current analysis. The disadvantage is that disaster frequency conflates major disasters that involve high human or economic losses with more numerous, much smaller, loss events. Using the frequency of disasters in the analysis, as opposed to the magnitude of losses, therefore, does not allow us to completely rule out that disaster losses may be higher globally during El Niño/La Niña events than at other times. In other words, the frequency of disasters could be independent of ENSO events, but the aggregate losses are higher during ENSO events, either due to higher average losses per disaster or, perhaps, because of exceptionally high losses in a few major disasters. As will be shown later, however, the global characteristics of local and regional precipitation anomalies during ENSO extremes suggest that the magnitude of hydrometeorological hazard events is *not* greater during El Niño/La Niña conditions than in neutral conditions.

The limitation that comes with employing disaster frequency, however, must be considered in light of the multiple disadvantages that come with the use of loss levels as the outcome variables of interest. None of the individual loss variables—mortality, the affected population, or economic losses—adequately characterizes losses associated with the different types of hydrometeorological hazard events, and these variables cannot be easily combined into a multivariate measure of disaster losses. Problems include missing data, a lack of standardized definitions and assessment methods, differences among loss variables in terms of how losses associated with different hydrometeorological hazards are reflected, the confounding roles of exposure and vulnerability in creating losses, and problems with respect to the attribution of losses to particular types of hydrometeorological hazard events.

A full inventory of losses in any given disaster may include not only mortality, but also economic losses across the range of social, productive, infrastructure, and environmental sectors. Loss patterns vary spatially. Disasters in poor countries tend to have higher death tolls than in rich countries. Gross economic losses per event are much higher in rich countries than in poor ones.

Data on aggregate economic losses in EM-DAT are limited. Only a third of the entries include estimates of economic losses, and the economic loss estimates that do exist are generally based on ad hoc reports rather than systematic, multisectoral assessments of combined direct losses to assets and indirect losses to production across all of the affected sectors.

For these reasons, neither mortality nor economic losses are adequate as a sole indicator of disaster magnitude. Another candidate variable, "affected people," is not defined well enough to constitute an unambiguous measure of losses. Therefore, insufficient information is available to adequately characterize the magnitude of disaster losses across all climatic hazards.

Finally, and in light of the role of vulnerability to disaster causality, loss attribution can be highly problematic. For example, unlike flooding, where people can be killed or property can be destroyed from the direct impact of exposure to water, the impact of drought on people is entirely mediated by the economy (see Sen 1981; Benson and Clay 1998). Drought-related mortality, when it occurs, is always a result of complex nature–society relationships in which socioeconomic conditions play a particularly important role in the outcome. This complicates the use of disaster losses as a variable in an analysis of the contributions of climatic factors to disaster causality.

Thus, the use of disaster frequency to measure the degree to which ENSO events affect loss patterns minimizes the influence of confounding factors, incomplete accounting of losses, and difficulties with the attribution of losses to particular causes. At the same time, it capitalizes on the fact that EM-DAT applies the same inclusion criteria every year, so that the same biases, in terms of the sources that are consulted, and inclusion criteria are standardized over the entire study period. Variations in loss levels partly depend on varying degrees of exposure and vulnerability. Frequency is less sensitive to variations in exposure and vulnerability

[1] "Affected" people are those requiring immediate assistance during a period of emergency; it can also be displaced or evacuated people.

than are losses for the purposes of assessing climatic contributions to disaster causality. Finally, frequency is a more robust metric than that of losses, considering the differential impacts of the different hazards being considered.

b. Rainfall data

Monthly to seasonally averaged precipitation anomalies are used to investigate the climate side of the hydrometeorological disasters. Clearly, droughts occur on these climate time scales, and longer. Similarly, though, positive precipitation anomalies, which may be experienced as weather anomalies, that are aggregated over time lead to the regional flooding that then registers as a national disaster. Even extreme weather events such as hurricanes demonstrate interannual variability in strength and frequency of occurrence, contributing to seasonally averaged precipitation anomalies.

Gridded precipitation data over global land points is taken from two sources, due to uncertainties in such analyses. The first is the gridded analysis of the rain gauge data from the Global Historical Climatology Network (GHCN), which is available at 5° horizontal resolution from the National Climate Data Center (information available online at http://www.ncdc.noaa.gov/oa/climate/research/ghcn/ghcngrid.html). This dataset is based on 2064 homogeneity-adjusted precipitation stations (from the United States, Canada, and the former Soviet Union) that were combined with a dataset containing 20 590 raw precipitation stations throughout the world to create the gridded fields. In grid boxes with no homogeneity-adjusted data, GHCN raw data were used to provide the greatest possible global coverage. The second is the global land precipitation dataset of the Climate Research Unit (CRU) of the University of East Anglia (UEA; Hulme 1992, 1994), which is supplied at 2.5° x 3.75° horizontal resolution (information online at http://www.cru.uea.ac.uk/~mikeh/datasets/global). The station dataset on which this gridded dataset is based is an extension of the original CRU/U.S. Department of Energy (DoE) data described in Eischeid et al. (1991). The nearly 12 000 stations used were subjected to extensive quality control before incorporation into the gridded analysis.

Monthly mean precipitation totals are used only for the period of 1950–95. Rainfall anomalies for each set are calculated relative to the respective climatology covering the entire 46-yr period. The years 1950–95 constitute the analysis period also for the climate model results (section 2c) and the SSTs (i.e., Niño-3.4 ENSO index, section 2e). Although data for all of these variables are available for more recent years, the quality of the precipitation data limits the analysis to 1995. After that time, the aggregated rainfall values begin to diverge, showing unexplainable trends (in opposite directions, not shown), making both datasets suspect.

c. Rainfall forecasts

Three different atmospheric general circulation models (AGCMs) were forced with monthly mean observed SSTs for the period of 1950–95. Information on model resolution and ensemble size, as well as references to information on model physics, is provided in Table 1. The ensemble members from a particular AGCM differ from one another only in their initial atmospheric states at the beginning of the runs. Observed atmospheric initial conditions are not inserted at any time.

The seasonal (i.e., 3-month average) precipitation from the three AGCMs is transmuted into a single probabilistic forecast. The ensemble of integrations from each AGCM is converted into three-category probabilities for above-, near-, and below-normal seasonal precipitation, based on each model's historical terciles for precipitation over the 1950–95 period. The AGCM probabilistic rainfall predictions are then combined using a Bayesian approach (Rajagopalan et al. 2002), based on the regional and seasonal skill of each model, and a climatological forecast of equal probabilities for each category. The International Research Institute for Climate Prediction (IRI) currently employs this approach to multimodel ensembling for their probabilistic seasonal forecasts for temperature and precipitation. In terms of probabilistic measures, such as the ranked probability skill score (RPSS) and reliability, the IRI's Bayesian approach outperforms the individual models and also outperforms simpler model combination strategies, such as the straight pooling of all ensemble members (Barnston et al. 2003; Robertson et al. 2004).

These are technically multimodel AGCM simulations, however, they will be referred to as forecasts. Thus, the skill of these forecasts is "potential skill" because it assumes that the boundary conditions, such as SSTs, which force the predictable part of seasonal climate, are perfectly predictable.

d. Skill metric

The RPSS (Epstein 1969; Wilks 1995) quantifies the skill of the multimodel rainfall forecasts. The RPSS

TABLE 1. The three atmospheric GCMs used for the rainfall forecasts: the National Center for Atmospheric Research (NCAR) Community Climate Model, version 3.2 (CCM3.2; Hack et al. 1998; available online at http://www.mpimet.mpg.de/en/extra/models/echam/index.php); the ECHAM model, version 4.5 (ECHAM4.5; Roeckner et al. 1996); and the National Aeronautics and Space Administration's (NASA's) Seasonal-to-Interannual Prediction Project (NSIPP; online at http://nsipp.gsfc.nasa.gov/research/atmos/atmos_descr.html) at the Goddard Space Flight Center.

Model	CCM3.2	ECHAM4.5	NSIPP1
Ensemble size	10	24	9
Horizontal resolution	T42	T42	2.5° × 2.0°
Vertical resolution	18	19	34

measures the squared error between the cumulative forecast and observed probabilities (CP_F and CP_O, respectively), then weighs that score against a reference forecast of climatology, which is the historically observed frequency of occurrence in each category,

$$\mathrm{RPSS} = 100 \times \left(1 - \frac{\mathrm{RPS}_{\mathrm{fcst}}}{\mathrm{RPS}_{\mathrm{ref}}}\right), \tag{1}$$

where

$$\mathrm{RPS} = \sum_{m=1}^{\mathrm{Ncategories}} (\mathrm{CP}_{F_m} - \mathrm{CP}_{O_m})^2. \tag{2}$$

A score of 100% implies that the observed category is always forecast with 100% confidence. A score of 0 implies always, or effectively, forecasting climatological probablities, and a score of <0 means the forecast system performs worse than climatology. There is no analytical formula or lookup table for the statistical significance levels of the RPSS. One can estimate the level of significance for RPSS via a Monte Carlo resampling of the forecasts, but the RPSS is a stringent metric; forecasts drawn at random relative to the observed sequence of years typically yield a RPSS worse than that of climatological forecasts (Mason 2004). As a result, the Monte Carlo estimates of critical RPSS values, even at the 99% confidence level, are usually negative. Still, it is desirable to designate a level of skill deemed high and useable even if that designation is subjective. Thus, a RPSS skill threshold of 5% is chosen to represent "good skill" of the forecasts, because this value exceeds that of climatological forecasts and is substantially greater than that obtainable from random forecasts. In a discussion of the results, presented in section 5, "skillful forecasts" refers to those that meet or exceed the subjective RPSS threshold of 5%.

e. Definition of El Niño/La Niña conditions

The Niño-3.4 index, which is the average SST anomaly within the region 5°S–5°N, 170°–120°W, determines the categorical state of ENSO for the purposes of the analyses presented here. The Niño-3.4 index is one of the most widely used ENSO indices (Barnston et al. 1997) because of the prevailing effect of SST variability within this region on the global climate. The SST data are taken from version 2 of the extended reconstructed sea surface temperature (ERSST) dataset (Smith and Reynolds 2004).

The upper and lower 25% of the distribution of the monthly mean Niño-3.4 index delimit ENSO extremes; this categorization follows from the quasi-periodic recurrence of El Niño at about 4 yr. The middle 50% of the distribution refers to neutral conditions. Figure 1 illustrates this classification, which leads to the identification of El Niño and La Niña events that are largely consistent with existing lists (e.g., Trenberth 1997; Mason and Goddard 2001).

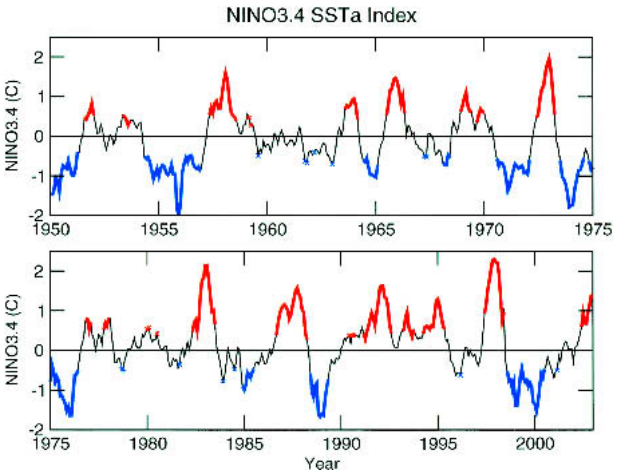

FIG. 1. Time series of the monthly mean Niño-3.4 index (SST anomaly averaged 5°S–5°N, 170°–120°W) (°C). El Niño and La Niña events are highlighted with bold red and blue lines, respectively. El Niño and La Niña conditions of insufficient duration to qualify as events are indicated by red and blue x's, respectively.

The language regarding ENSO is specific and deliberate in this manuscript. The term *ENSO* refers to the entire range of SST variability in the equatorial central/eastern Pacific Ocean, even though in a broader context it refers to the associated tropical Pacific atmospheric variability, and even to the global teleconnections. The terms *El Niño/La Niña conditions* and *ENSO extremes* indicate the upper and lower 25% of the distribution of Niño-3.4 values, which are evaluated at the monthly to seasonal time scale. The term *ENSO event* refers to the entire life span of an ENSO extreme, from its initiation, typically in the boreal spring/summer, to its demise, typically in the following spring. For the purposes of our analyses, El Niño or La Niña conditions must exist for at least five consecutive months to qualify as an event.

3. Frequency of disasters

Because data within EM-DAT have been consistently reported over the past 25–30 yr, it can serve as a baseline against which to assess the influence of ENSO events on certain types of socioeconomic losses. The upward trend in disaster frequency, the most obvious feature of the time series (Fig. 2a), reflects some combination of the following: the increased reporting of disasters, greater concentrations of people and wealth in high-risk areas, increasing vulnerability, and long-term changes in the frequency or severity of climatic hazard events. This trend is removed by fitting a second-order polynomial to the yearly data on a disaster frequency; the detrended time series is used for the analysis of disaster frequencies relative to ENSO events.

If one assumes for the moment that all hydrometeo-

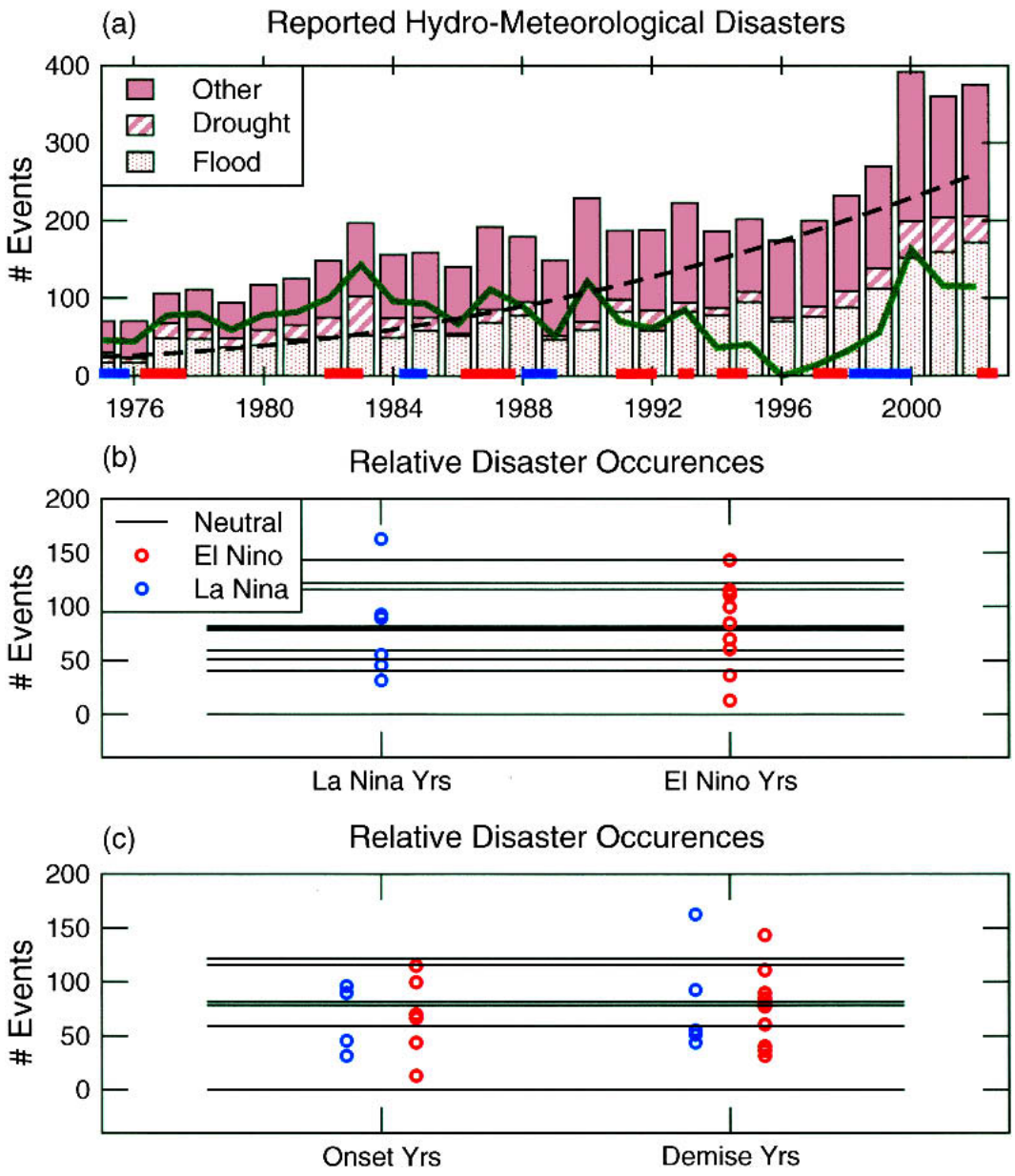

FIG. 2. (a) Reported hydrometeorological disasters. Relative incidences of floods (dotted), droughts (hatched), and "other" (brown), which include windstorms and temperature extremes, are demarcated. El Niño (thick red lines) and La Niña (thick blue lines) events, consistent with those shown in Fig. 1, are indicated along *x* axis. Solid green line represents time series of total disaster occurrence, detrended using a second-order polynomial (black dashed line). (b) Relative disaster occurrences using detrended time series shown in (a) for calendar years that experienced six or more months of El Niño or La Niña conditions (red and blue circles, respectively) as determined by the thick red and blue lines from (a), and listed in Table 2. The years that contained more than 6 months of neutral conditions serve as the baseline (horizontal black lines). (c) Similar to (b), except for the onset and demise years of El Niño (red circles) and La Niña (blue circles). The years that contain no months within the intervals of El Niño or La Niña events serve as the baseline (horizontal black lines).

rological hazard events in years of ENSO extremes arise from El Niño or La Niña, the question then becomes, "How is the disaster frequency in years of El Niño/La Niña different from that in neutral years?". One would like to examine disaster frequencies over the precise duration of El Niño or La Niña conditions; however, particularly for drought data, information regarding the specific month(s) is often not recorded in EM-DAT. ENSO events are rarely contained in a calendar year; they typically begin in the boreal spring/summer of one year, peak in the winter, and subsequently decay the following year. Consequently, the

TABLE 2. Years associated with analysis presented in Fig. 2, based on the Niño-3.4 index shown in Fig. 1. "Dominant conditions" are indicated if more than 6 months in the calendar year meet the categorical criterion. An "event" is identified as El Niño/La Niña conditions occurring for at least four consecutive months, in which case the beginning year of the interval is the "onset" year, and the ending (or subsequent) years are the "demise" years.

El Niño		La Niña		Neutral
Dominant conditions	Event onset/demise	Dominant conditions	Event onset/demise	Dominant conditions
	1976/1977	1975	1975/1976	1977
	1977/1978	1985	1984/1985	1978
1982	1982/1983	1988	1988/1989	1979
1983		1998	1998/1999, 2000	1980
1987	1986/1987, 1988	1999		1981
1991	1991/1992	2000		1984
1992				1989
1993				1990
1994	1994/1995			1995
1997	1997/1998			1996
2002	2002/2003			2001

* Even though it qualifies as an event, 1993 is not included in the El Niño onset/demise column because it began and ended in the same calendar year.

relative disaster frequency during El Niño/La Niña is analyzed using two definitions of ENSO event years. First, each year is categorized as El Niño, La Niña, or neutral, depending on which condition was predominant (i.e., existed for more than 6 months of the year) (Fig. 2b, Table 2). Second, relative disaster frequencies in the year of onset and year(s) of demise for actual ENSO events are considered relative to years with no onset or demise (Fig. 2c, Table 2).

Interannually, in either case, the number of hydrometeorological-related disasters appears to be largely insensitive to the occurrence of ENSO extremes (Figs. 2b,c). The Kolmogorov–Smirnov test, which was employed to compare the distributions of disaster frequencies in neutral years against those in El Niño or La Niña years, or against those in the onset/demise years of ENSO events, does not reject the null hypothesis that these data are drawn from the same population at the 95% confidence level. A similar result is obtained for testing differences in the means by using a nonparametric version of the *t* test. Globally, the number of flood disasters within EM-DAT exhibits no consistent relationship to ENSO events (Fig. 2a). Drought disasters, on the other hand, do tend to occur more frequently in selected regions during the demise year(s) of El Niño events (Fig. 2a; Dilley and Heyman 1995; Bouma et al. 1997; Thomson et al. 2003). But, overall, hydrometeorological disasters experienced globally during El Niño and La Niña events are statistically not significantly different from what is experienced in neutral years. Disasters and associated losses occur in all years.

4. Precipitation anomalies and ENSO events

Moreover, not all disasters, or the climate anomalies contributing to them, during ENSO events are due to the ENSO event. The body of research documenting and describing El Niño/La Niña and their effects on global and regional climate has grown considerably in the last several decades (McPhaden et al. 1998; Trenberth et al. 1998; Wallace et al. 1998). The claim that El Niño may be predictable up to a year in advance[2] (Cane et al. 1986), and the recognition that it yields somewhat repeatable patterns of anomalous climate, has fueled this wealth of research. These factors have also provided an impetus for seasonal climate forecasting efforts (Goddard et al. 2001). One thing the climate community has learned, however, is that the effects of El Niño/La Niña are region specific. Observational studies of the last 50+ yr indicate that only approximately 20%–30% of land areas experience statistically significant repeatability in the occurrence of categorical precipitation anomalies during ENSO extremes in any particular season (Mason and Goddard 2001). However, due to such factors as differences in the timing and patterns of ENSO events, climate variability forced by SST anomalies in the tropical Atlantic and tropical Indian Oceans that is independent of ENSO, and inherent uncertainty due to the internal chaotic dynamics of the atmosphere, the expected climate anomalies may not occur during every El Niño or La Niña event for every region.

To determine whether climate anomalies, in particular, precipitation anomalies, become more severe or widespread during ENSO events, a precipitation perturbation index (PPI) is developed,

$$\mathrm{PPI}(t) = \int\int \frac{|P'(x, y, t)|}{S_{P'}(x, y, t)}\, dxdy, \tag{3}$$

where $S_{P'}(x,y)$ is the standard deviation of the precipitation anomalies for a given calendar month, $P'(x,y,t)$,

[2] In practice the useable lead time for these forecasts is much shorter than the early optimistic claims of 1 yr (e.g., Landsea and Knaff 2000).

at each grid point, (x,y). The PPI is an absolute value measure. It represents an integral of normalized anomalous precipitation magnitude, or, equivalently, the number of standard deviations that the local precipitation departs from the local normal. In this analysis the PPI is integrated over low-latitude (30°S–30°N) land points (Fig. 3), although the integral over global land points (not shown) yields identical results. The PPI indicates the overall perturbation to rainfall patterns; positive and negative precipitation anomalies in different parts of the world do not cancel one another out. For purposes of presentation and correlation with ENSO indices, the resulting time series for the PPI has been normalized to have zero mean and unit variance relative to the monthly mean annual cycle for the 1950–95 period.

The PPI does not correlate with ENSO indices, such as Niño-3.4 (Fig. 3a). Because the PPI is an absolute value measure of rainfall anomalies, the time series is

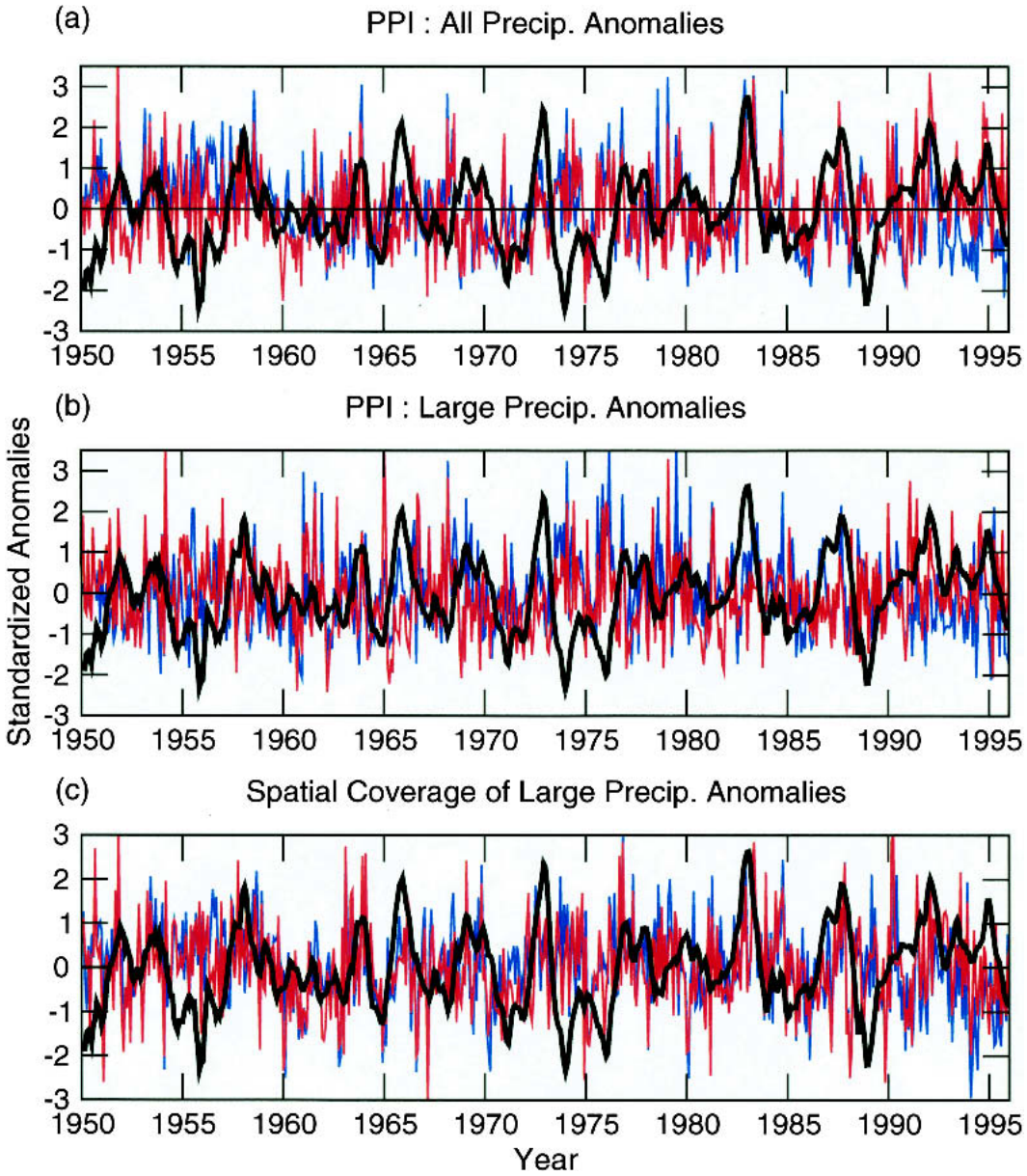

FIG. 3. PPI integrated over low latitudes (30°S–30°N) from two observed precipitation datasets (red: UEA CRU and blue: GHCN). (a) PPI using all land points, and (b) PPI using a subset of land points for which the magnitude of precipitation anomalies exceeds 1σ. (c) Number of grid points for which the magnitude of the precipitation anomaly exceeds 1σ. Niño-3.4 index of ENSO is plotted for comparison in each graph (black). All time series have been normalized to have zero mean and unit variance relative to the monthly mean annual cycle over the 1950–95 period.

compared against the absolute value of Niño-3.4 also, which can be interpreted as the magnitude of forcing from the tropical Pacific. The PPI does not correlate with the absolute value of Niño-3.4 either.

Two similar analyses are carried out with variations on the PPI, comparing the perturbation time series against Niño-3.4 and its absolute value. Both cases focus on more extreme rainfall impacts, with similar results. In the first case, the PPI considers only land points for which the magnitude of the normalized anomaly exceeds one standard deviation (Fig. 3b); this variant focuses on the overall severity of extreme anomalies. One could imagine the possibility that the PPI was relatively constant over time, resulting from spatially concentrated extreme precipitation anomalies during El Niño/La Niña conditions and weaker, but more widespread, anomalies during neutral years. When including in the PPI only the extreme precipitation anomalies, these potential differences between El Niño/La Niña and neutral conditions would be highlighted. The other case counts the number of land points for which the normalized anomaly exceeds one standard deviation (Fig. 3c); this variant focuses on the relative spatial coverage of extreme anomalies but not their magnitude. In both cases, the resulting precipitation time series bears no correlation to the occurrence or magnitude of ENSO extremes.

Although other research suggests that the spatial extent of below-normal rainfall increases in response to El Niño events (Lyon 2004, manuscript submitted to *J. Climate*), leading to an increase in reported drought disasters in some regions (Dilley and Heyman 1995; Bouma et al. 1997), in other years equivalently anomalous precipitation is observed in the same or different parts of the world. No linear relationship exists between ENSO extremes and the overall frequency or severity of precipitation anomalies. That does not necessarily mean that ENSO extremes have no influence on the overall frequency or severity of precipitation anomalies.

Distributions of the rainfall indices relative to the Niño-3.4 index of ENSO do show a discernible, though subtle, change during El Niño and La Niña conditions compared to neutral conditions (Fig. 4). The clearest shift in the frequency distribution exists for the PPI of all anomalies (Fig. 4a2), but this shift represents an increase of only about 3%–4% in the mean relative to the neutral conditions (Table 3). For the PPI of large anomalies, the distributions during El Niño and neutral conditions are statistically indistinguishable at the 95% confidence level, according to the Kolmorgorov–Smirnov test; and for the spatial coverage of large precipitation anomalies, the two rainfall datasets give differing results for the uniqueness of the frequency distribution under La Niña conditions compared to that of neutral conditions (Table 3).

A relevant finding illustrated in Fig. 4 is that the largest values of the rainfall indices are not greater during ENSO extremes than during neutral conditions. Changes in the expected frequency of "high" values of the indices (i.e., exceeding $+1\sigma$) are also small (Table 4), typically at only a few percent. The largest differences between neutral and El Niño/La Niña conditions exists in the "low" tail of the distribution, with overall less perturbation more likely under neutral conditions compared to ENSO extremes. La Niña conditions lead to the most notable increase in the frequency of high values—those for the PPI of large anomalies (20% compared to the ~14% observed under neutral conditions). The high values of the precipitation indices are of primary concern because these indicate the greatest potential for climatic hazard events. Although ENSO extremes do modify the expected frequencies of those high values relative to neutral conditions, the difference is small. The risk of severe and/or widespread rainfall anomalies under neutral conditions remains comparable to that during ENSO extremes.

This is not intended to discount the devastating climatic hazard events during El Niño and La Niña events that frequently occur in ENSO teleconnection regions (Ropelewski and Halpert 1987; Ropelewski and Halpert 1989; Mason and Goddard 2001), such as the droughts over parts of southern Africa and southeastern Asia and the excessive rainfall and flooding over southeastern South America and parts of the Great Horn of Africa during El Niño events. Many countries of the world have come to expect adverse climate conditions from El Niño/La Niña events, which in many cases lead to loss of life and property. But because the aggregate rainfall anomalies do not change much during ENSO events, adverse climate conditions will occur somewhere in all years.

5. Climate predictability and ENSO events

The big difference during ENSO events is that climate forecasts are potentially more skillful at those times, as is demonstrated below for the 1950–95 period. Similar conclusions were reached by Branković and Palmer (2000) and Shukla et al. (2000) based on the predictability of 500-mb heights in the Northern Hemisphere. However, the current analysis arrives at that conclusion from a different perspective, and for a far more socially relevant variable (i.e., precipitation).

The first point is that, relative to neutral conditions, skillful forecasts can be made for a greater proportion of land areas during El Niño/La Niña conditions (Fig. 5). The percent of land area for which precipitation forecasts achieve good skill (i.e., where RPSS exceeds 5%, see section 2d) increases markedly in all seasons. However, the greatest relative increases appear near the end of the year, when ENSO events typically reach their peak magnitude. At that time, the amount of land areas for which forecasts potentially have good skill doubles, globally, during ENSO extremes relative to neutral conditions.

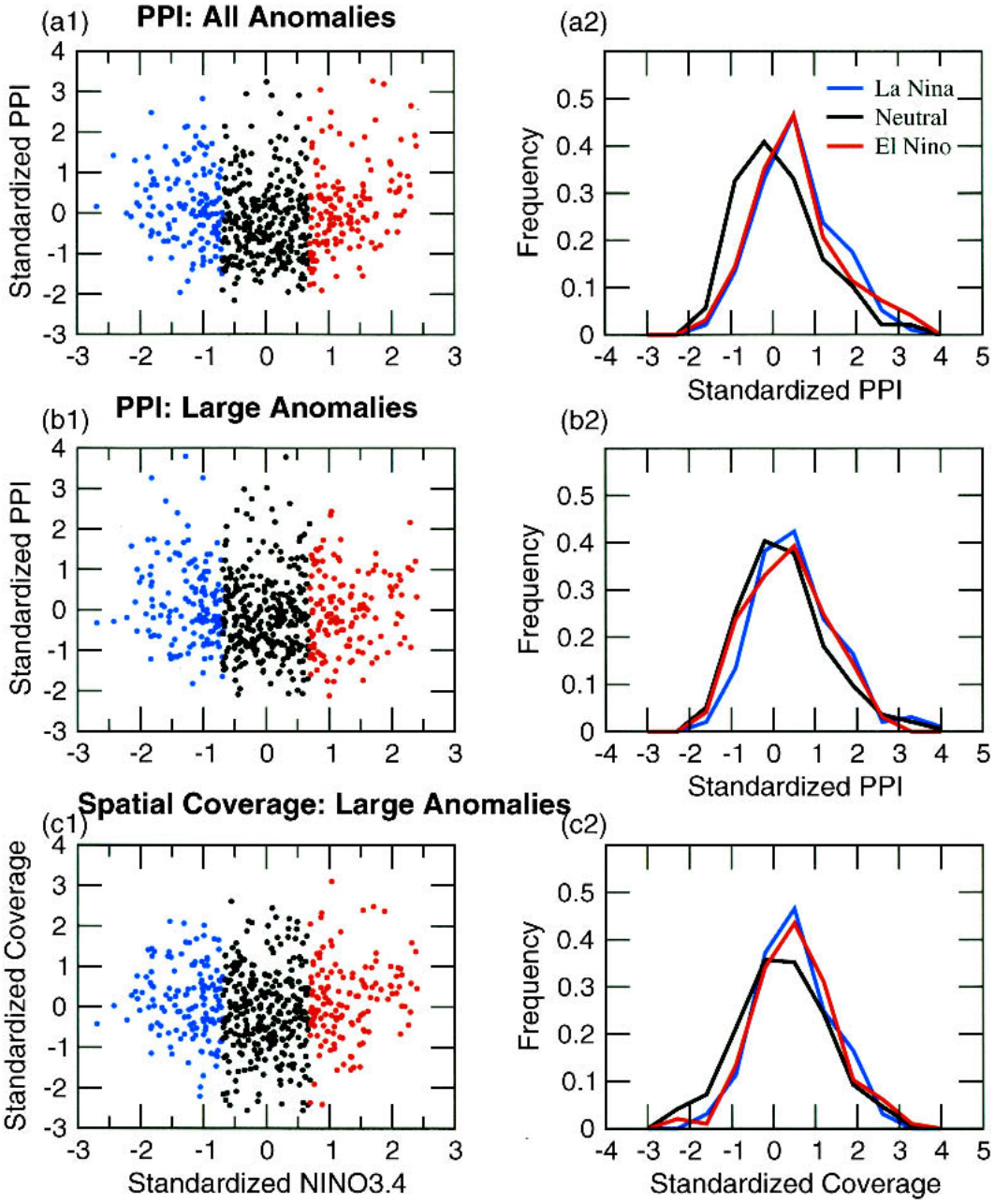

FIG. 4. Distribution of rainfall indices relative to ENSO category, using the UEA CRU rainfall data. (a1) Scatterplot of monthly mean PPI index calculated over all low-latitude land points (30°S–30°N) vs monthly mean ENSO category (La Niña conditions: blue; neutral conditions: black; El Niño conditions: red). (a2) Associated normalized frequency distributions of PPI values shown in (a1) in each ENSO category. (b1), (b2) Similar to (a1) and (a2), except that the PPI integration includes only those rainfall anomalies exceeding 1σ magnitude. (c1), (c2) Similar to (b1) and (b2), except the index quantifies relative spatial coverage of rainfall anomalies exceeding 1σ magnitude rather than their strength. All data have been normalized to have zero mean and unit variance relative to the monthly mean annual cycle over the 1950–95 period. A similar figure based on GHCN rainfall data, not shown, is nearly identical.

The second point is that where general predictability of the climate exists, forecast skill increases as ENSO extremes become stronger (Fig. 6). Seasonal climate consists of "signal," due to the boundary forcing primarily from changing SST patterns (e.g., Goddard et al. 2001), and "noise," due to the chaotic influences of the atmosphere's internal dynamics. As El Niño or La Niña conditions become stronger, the signal becomes more

TABLE 3. Results from the Kolmogorov–Smirnov (KS) test for uniqueness of sample distributions (1 = can reject null hypothesis that sample populations are effectively the same, at the 95% confidence level), and percent difference in the population mean for ENSO extremes relative to neutral conditions. The first value is based on monthly mean gridded rainfall data from UEA CRU; the second parenthetical value is based on GHCN gridded rainfall data.

	All P′ (PPI)		Extreme P′ (PPI)		Extreme P′ (spatial coverage)	
	KS test	Mean diff (%)	KS test	Mean diff (%)	KS test	Mean diff (%)
El Niño vs neutral	1 (1)	3.5 (4.5)	0 (0)	0.6 (−0.8)	1 (1)	3.8 (6.0)
La Niña vs neutral	1 (1)	3.6 (2.3)	1 (1)	1.9 (1.9)	1 (0)	3.4 (1.5)

discernible relative to the noise, and the likelihood for experiencing an "expected" climate anomaly due to the ENSO extreme becomes greater.

The linear relationship between the strength of the Niño-3.4 index and the probabilistic skill of three categories of rainfall forecasts calculated over global land areas exceeds the 99% confidence level[3] for statistical significance in all seasons for both positive and negative values of Niño-3.4 [e.g., the October–November–December (OND) season shown in Fig. 6]. The increase in average forecast skill during ENSO extremes relative to ENSO neutral conditions is 99% statistically significant[4] in all seasons, except for July–August–September (JAS) during El Niño conditions where the difference only exceeds the marginal significance of 90%. In general, the difference in forecast skill between La Niña and El Niño events is not significant. Furthermore, within the El Niño category, the linear relationship between forecast skill and El Niño strength exceeds 99% significance in all seasons. The linear relationship between forecast skill and La Niña strength exceeds the 97.5% level of significance during OND, when events tend to peak, and during January–February–March (JFM), when events are weakening, but atmospheric noise, particularly in the Northern Hemisphere extratropics, is relatively low (Kumar and Hoerling 1998). Even over areas without robust El Niño/La Niña teleconnections, climate predictions benefit from a stronger signal-to-noise ratio during ENSO extremes (Fig. 6b).

Much of the increase in overall forecast skill (Fig. 6a) during ENSO events results from increases in regional skill over places that exhibit a statistically significant repeatability in precipitation response to ENSO events (Fig. 6c, Fig. 7; Mason and Goddard 2001). For example, the forecasts exhibit substantially higher skill for ENSO events in JFM over Hawaii, the southern tier of the United States, southern Africa, eastern China, and the Philippines; in April–May–June (AMJ) over northeastern Brazil and the southern and central United States; in JAS over the Caribbean, western Sahel, Indonesia, and Australia; and in OND over Indonesia, eastern Africa, southeastern Brazil, the southern United States, and Mexico. Given the difficulty in determining the statistical significance of RPSS, however, these maps of skill improvement (Fig. 7) should be interpreted qualitatively. The weak and incoherent appearance of the negative regions infers little change in the skill owing to El Niño/La Niña. For the few semicoherent regions of reduced skill, such as parts of Indonesia and the northern part of the United States for OND, it is likely that forecast skill actually degrades during ENSO extremes for the forecast methodology applied here. Where coherent regions show improvement, particularly for differences in the RPSS that exceed 10%, one can assume that the seasonal forecasts will perform better during ENSO extremes.

These results (Figs. 6 and 7) constitute an approximate upper limit in forecast skill for seasonal precipitation because the dynamical models' atmospheres were forced with observed SSTs. In a real forecast setting skills decrease because imperfect SST predictions introduce additional uncertainty. At this time the most skillful SST predictions are for the tropical Pacific (i.e., for El Niño/La Niña). So, actual forecast skill will decrease even more during neutral conditions than during ENSO extremes. Thus, the increase in skill during ENSO events, that is realizable in practice is underestimated here. Increasing attention is being focused on predictions for the other tropical ocean basins, as the importance of accurate SSTs in the tropical Indian and Atlantic Oceans for dynamical climate prediction becomes recognized (Goddard and Graham 1999; Goddard and Mason 2002). At this time, most of the forecast skill that resides in these basins is that due to changes associated with ENSO (Penland and Matrosova 1998). Less observational data exist for the tropical Atlantic and Indian Oceans, and less is understood about the dynamics of interannual variability in these basins that are independent of ENSO. Thus, considerable room for improvement remains for SST predictions in these regions.

6. Summary and discussion

Conclusions from the above analysis for global, or even tropical, scales include the following:

[3] Statistical significance of linear relationships is based on the Pearson product-moment correlation coefficient, testing the null hypothesis that the correlation coefficient differs from 0.

[4] Statistical significance of difference in means or medians is based on the Mann–Whitney U test, a nonparametric analog of the *t* test.

TABLE 4. Observed frequencies of categorical monthly mean rainfall indices (Low: $\leq -1\sigma$; $-1\sigma <$ Med $< 1\sigma$; High: $\geq 1\sigma$) under El Niño, La Niña, and neutral conditions. The first value is based on gridded rainfall data from UEA CRU; the second parenthetical value is based on GHCN gridded rainfall data.

	All P′ (PPI)			Extreme P′ (PPI)			Extreme P′ (spatial coverage)		
	Low	Medium	High	Low	Medium	High	Low	Medium	High
El Niño	11% (10%)	72% (68%)	17% (22%)	17% (16%)	68% (77%)	15% (7%)	9% (8%)	75% (71%)	16% (21%)
Neutral	23% (19%)	65% (69%)	12% (12%)	17% (15%)	70% (70%)	13% (15%)	20% (17%)	66% (71%)	14% (12%)
La Niña	10% (9%)	70% (78%)	20% (13%)	10% (10%)	70% (72%)	20% (19%)	9% (11%)	72% (78%)	19% (11%)

- Overall perturbation to precipitation over land areas is only weakly affected by ENSO extremes. The risk of widespread extreme precipitation anomalies during ENSO extremes is comparable to that during neutral conditions. Furthermore, the highest values of integrated rainfall perturbation are not greater during ENSO extremes than during neutral conditions.
- The frequency of reported climate-related disasters does not increase during El Niño/La Niña years relative to neutral years. The degree to which overall losses may increase during ENSO events has not been estimated, but in the absence of increases in the magnitude of global aggregate climate anomalies during ENSO events any such increases would be due to socioeconomic, rather than climatic, causal factors.
- Forecast skill of seasonal rainfall increases, in magnitude and coverage, during ENSO extremes.

It is hoped that these results will motivate further analysis and improved representation of El Niño/La Niña–related climatic hazards and associated disasters. Disasters occurring during ENSO extremes must be discussed within the context of baselines, such as disaster occurrences in previous years and in neutral years. More effort should be given to understanding the attribution of disaster causality; would they have occurred in the absence of the ENSO event? More comprehensive and precise disaster databases and more comprehensive estimates of losses will aid in such research. Also, positive benefits of ENSO extremes should be more carefully documented, yielding a more complete

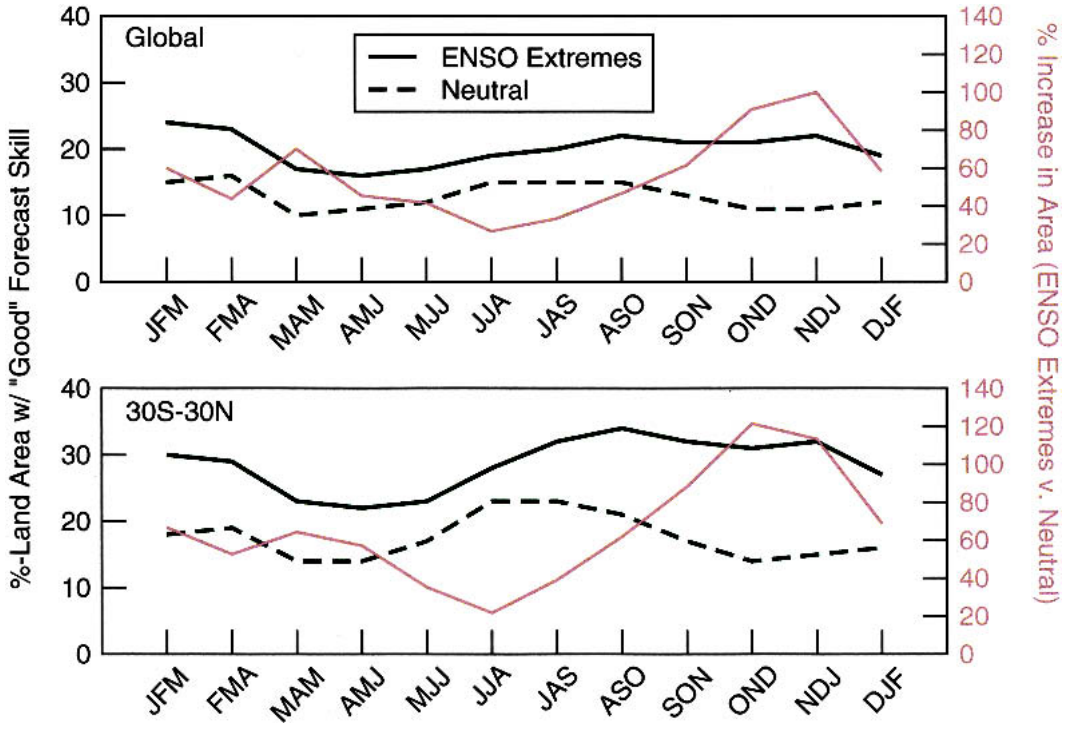

FIG. 5. Percentage of land area over which seasonal precipitation forecasts exhibit "good skill" (see section 2d) as measured by RPSS over the 1950–95 period. (top) RPSS that is averaged globally, and (bottom) RPSS that is averaged over low latitudes (30°S–30°N), for ENSO extremes (solid black), and neutral conditions (dashed black). Gray line (right scale) indicates the relative increase in land area for which good skill exists in ENSO extremes vs neutral conditions.

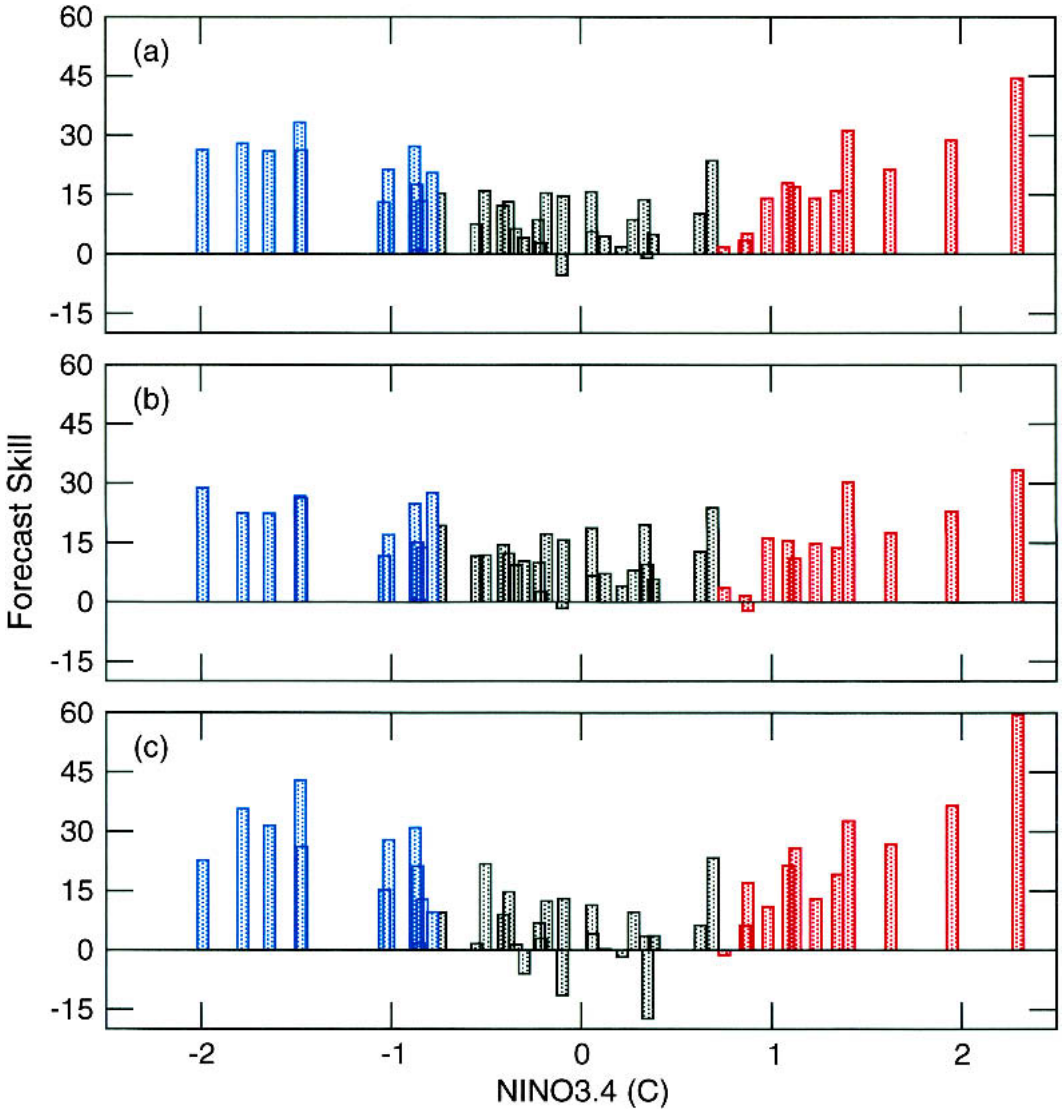

FIG. 6. Forecast skill (RPSS) for three categories of forecasts of OND rainfall for the 1950–95 period. Skill scores for each year are ordered by the corresponding OND Niño-3.4 index. (a) RPSS is calculated globally over land points for which the temporal RPSS over all years exceeds 5%. (b) Similar to (a), but including only those points with *no* statistically significantly repeatability of climate response to El Niño/La Niña. (c) Similar to (a), but including only those points with statistically significantly repeatability of climate response to El Niño/La Niña. Bars are color-coded by their respective category: La Niña (blue), neutral (black), and El Niño (red).

appreciation of the socioeconomic impacts of El Niño and La Niña events. Finally, increased efforts should be directed toward improving seasonal climate prediction capabilities for neutral ENSO conditions, because overall rainfall perturbations can be just as great as during ENSO extremes.

At this time, given that society is faced with climate-related disasters in all years, seasonal climate forecasts can make a targeted contribution to reducing the associated losses. Because overall forecast skill is highest during El Niño/La Niña, advanced warning that an ENSO event is likely to develop and reliable climate forecasts for regions that are likely to be affected allows international, regional, and national agencies and local communities to prepare. Vulnerability reduction can potentially reduce the frequency and severity of hydrometeorological disasters incurred in those years. The United States realized such a reduction in adverse impacts during the 1997/98 El Niño event; California estimated a 1 billion dollar savings in property damages due to better preparedness in response to seasonal climate forecasts (Chagnon 1999; Weiher 1999). Furthermore, beneficial effects of ENSO have also been noted. For example, tropical Atlantic hurricanes that threaten the southeastern United States, the Caribbean, and eastern Central America occur less frequently during

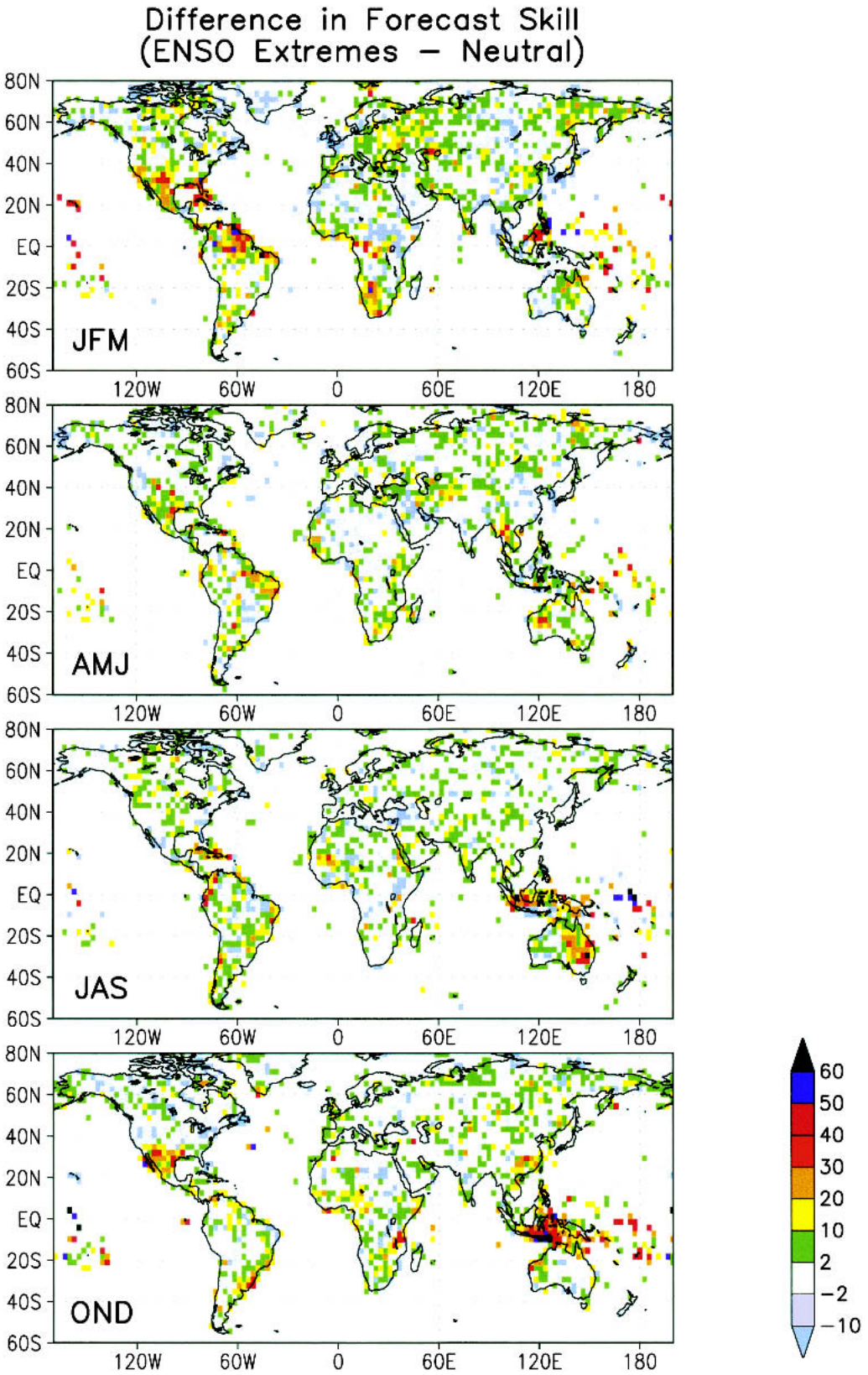

FIG. 7. Differences in skill (RPSS) for three categories of seasonal rainfall forecasts between ENSO extremes and neutral conditions for the 1950–95 period. Positive values indicate higher skill during ENSO extremes.

El Niño years (Gray 1984). Also, warmer winter temperatures commonly are observed in the northern United States during El Niño, leading to less energy use and, therefore, lower energy prices (Chagnon 1999). Thus, between mitigating adverse climate effects and taking advantage of beneficial ones through the prudent use of climate forecasts, El Niño and La Niña years may eventually result in substantially lower socioeconomic losses, globally, than are realized in other years.

Acknowledgments. The authors thank Mark Cane, Dave DeWitt, Simon Mason, Tony Barnston, Kevin Trenberth, and two anonymous reviewers for comments on this work. The authors are supported by a cooperative agreement from the National Oceanic and Atmospheric Administration (NOAA) NA07GP0213. The views expressed herein are those of the authors and do not necessarily reflect the views of NOAA or any of its subagencies.

REFERENCES

Barnston, A. G., M. Chelliah, and S. B. Goldenberg, 1997: Documentation of a highly ENSO-related SST region in the equatorial Pacific. *Atmos.–Ocean,* **35,** 367–383.

——, S. J. Mason, L. Goddard, D. G. DeWitt, and S. E. Zebiak, 2003: Increased automation and use of multimodel ensembling in seasonal climate forecasting at the IRI. *Bull. Amer. Meteor. Soc.,* **84,** 1783–1796.

Benson, C., and E. J. Clay, 1998: The impact of drought on subsaharan African economies: A preliminary examination. The World Bank Tech. Paper 401, 80 pp.

Bouma, M. J., R. S. Kovats, S. A. Goubet, J. S. H. Cox, and A. Haines, 1997: Global assessment of El Niño's disaster burden. *Lancet,* **350,** 1435–1438.

Branković, Č., and T. N. Palmer, 2000: Seasonal skill and predictability of ECMWF PROVOST ensembles. *Quart. J. Roy. Meteor. Soc.,* **126,** 2035–2067.

Cane, M. A., S. C. Dolan, and S. E. Zebiak, 1986: Experimental forecasts of El Niño. *Nature,* **321,** 827–832.

Chagnon, S. A., 1999: Impacts of 1997–98 El Niño generated weather in the United States. *Bull. Amer. Meteor. Soc.,* **80,** 1819–1828.

Dilley, M., and B. N. Heyman, 1995: ENSO and disaster: Droughts, floods and El Niño/Southern Oscillation warm events. *Disasters,* **19,** 181–193.

Eischeid, J. K., H. G. Diaz, R. S. Bradley, and P. D. Jones, 1991: A comprehensive precipitation data set for global land areas. U.S. Department of Energy Carbon Dioxide Research Division Tech. Rep. TR051, 81 pp.

EM-DAT, cited 2003: The OFDA/CRED international disaster database. Université Catholique de Louvain. [Available online at http://www.cred.be.]

Epstein, E. S., 1969: A scoring system for probability forecasts of ranked categories. *J. Appl. Meteor.,* **8,** 985–987.

Goddard, L., and N. E. Graham, 1999: The importance of the Indian Ocean for simulating rainfall anomalies over eastern and southern Africa. *J. Geophys. Res.,* **104,** 19 099–19 116.

——, and S. J. Mason, 2002: Sensitivity of seasonal climate forecasts to persisted SST anomalies. *Climate Dyn.,* **19,** 619–631.

——, ——, S. E. Zebiak, C. F. Ropelewski, R. Basher, and M. A. Cane, 2001: Current approaches to seasonal-to-interannual climate predictions. *Int. J. Climatol.,* **21,** 1111–1152.

Gray, W. M., 1984: Atlantic seasonal hurricane frequency. Part I: El Niño and 30 mb quasi-biennial oscillation influences. *Mon. Wea. Rev.,* **112,** 1649–1668.

Hack, J. J., J. T. Kiehl, and J. W. Hurrell, 1998: The hydrologic and thermodynamic characteristics of the NCAR CCM3. *J. Climate,* **11,** 1179–1206.

Hulme, M., 1992: A 1951–80 global land precipitation climatology for the evaluation of General Circulation Models. *Climate Dyn.,* **7,** 57–72.

——, 1994: Validation of large-scale precipitation fields in general circulation models. *Global Precipitations and Climate Change*, M. Desbois and F. Desalmand, Eds., NATO ASI Series, Springer-Verlag, 387–406.

Kumar, A., and M. P. Hoerling, 1998: Annual cycle of Pacific–North American seasonal predictability associated with different phases of ENSO. *J. Climate,* **11,** 3295–3308.

Landsea, C. W., and J. A. Knaff, 2000: How much skill was there in forecasting the very strong 1997–98 El Niño? *Bull. Amer. Meteor. Soc.,* **81,** 2107–2120.

Mason, S. J., 2004: On using "climatology" as a reference strategy in the Brier and ranked probability skill scores. *Mon. Wea. Rev.,* **132,** 1891–1895.

——, and L. Goddard, 2001: Probabilistic precipitation anomalies associated with ENSO. *Bull. Amer. Meteor. Soc.,* **82,** 619–638.

McPhaden, M. J., and Coauthors, 1998: The Tropical Ocean-Global Atmosphere observing system: A decade of progress. *J. Geophys. Res.,* **103,** 14 169–14 240.

Penland, C., and L. Matrosova, 1998: Prediction of tropical Atlantic sea surface temperatures using linear inverse modeling. *J. Climate,* **11,** 483–496.

Rajagopalan, B., U. Lall, and S. E. Zebiak, 2002: Categorical climate forecasts through regularization and optimal combination of multiple GCM ensembles. *Mon. Wea. Rev.,* **130,** 1792–1811.

Robertson, A. W., U. Lall, S. E. Zebiak, and L. Goddard, 2004: Improved combination of multiple atmospheric GCM ensembles for seasonal prediction. *Mon. Wea. Rev.,* **132,** 2732–2744.

Roeckner, E., and Coauthors, 1996: The atmospheric general circulation model ECHAM4: Model description and simulation of present-day climate. Max-Planck-Institüt für Meteorologie Rep. 218, 90 pp.

Ropelewski, C. F., and M. S. Halpert, 1987: Global and regional scale precipitation patterns associated with the El Niño/Southern Oscillation. *Mon. Wea. Rev.,* **115,** 1606–1626.

——, and ——, 1989: Precipitation patterns associated with the high index phase of the Southern Oscillation. *J. Climate,* **2,** 268–284.

Sen, A. K., 1981: *Poverty and Famines: An Essay on Entitlement and Deprivation*. Clarendon Press, 257 pp.

Shukla, J., and Coauthors, 2000: Dynamical seasonal prediction. *Bull. Amer. Meteor. Soc.,* **81,** 2593–2606.

Smith, T. M., and R. W. Reynolds, 2004: Improved extended reconstruction of SST (1854–1997). *J. Climate,* **17,** 2466–2477.

Sponberg, K., 1999: Navigating the numbers of climatological impact. Compendium of Climatological Impacts, University Corporation for Atmospheric Research, Vol. 1, National Oceanic and Atmospheric Administration, Office of Global Programs, 13 pp. [Available online at http://www.cip.noaa.gov/docs/navimpact.pdf.]

Thomson, M. C., K. Abayomi, A. G. Barnston, M. Levy, and M. Dilley, 2003: El Niño and drought in southern Africa. *Lancet,* **361,** 437–438.

Trenberth, K. E., 1997: The definition of El Niño. *Bull. Amer. Meteor. Soc.,* **78,** 2771–2777.

——, G. W. Branstator, D. Karoly, A. Kumar, N.-C. Lau, and

C. F. Ropelewski, 1998: Progress during TOGA in understanding and modelling global teleconnections associated with tropical sea surface temperatures. *J. Geophys. Res.,* **103,** 14 291–14 324.

UCAR, 1994: El Niño and climate prediction. Reports to the Nation on our Changing Planet, UCAR, No. 3, 25 pp.

Wallace, J. M., E. M. Rasmusson, T. P. Mitchell, V. E. Kousky, E. S. Sarachik, and H. von Storch, 1998: On the structure and evolution of ENSO-related climate variability in the tropical Pacific: Lessons from TOGA. *J. Geophys. Res.,* **103,** 14 241–14 259.

Weiher, R. F., Ed., 1999: Improving El Niño forecasting: The potential benefits. U.S. Dept. of Commerce, National Atmospheric and Oceanic Administration, 57 pp. [Available online at http://www.publicaffairs.noaa.gov/worldsummit/pdfs/improving.pdf.]

Willks, D. S., 1995: *Statistical Methods in the Atmospheric Sciences*. Academic Press, 467 pp.